

Stochastic Gradient Descent with Large Learning Rate

Kangqiao Liu*, Liu Ziyin*, Masahito Ueda
Department of Physics, University of Tokyo

November 1, 2021

Abstract

As a simple and efficient optimization method in deep learning, stochastic gradient descent (SGD) has attracted tremendous attention. In the vanishing learning rate regime, SGD is now relatively well understood, and the majority of theoretical approaches to SGD set their assumptions in the continuous-time limit. However, the continuous-time predictions are unlikely to reflect the experimental observations well because the practice often runs in the large learning rate regime, where the training is faster and the generalization of models are often better. In this paper, we propose to study the basic properties of SGD and its variants in the non-vanishing learning rate regime. The focus is on deriving exactly solvable results and relating them to experimental observations. The main contributions of this work are to derive the stable distribution for discrete-time SGD in a quadratic loss function with and without momentum. Examples of applications of the proposed theory considered in this work include the approximation error of variants of SGD, the effect of mini-batch noise, the escape rate from a sharp minimum, and the stationary distribution of a few second order methods.

1 Introduction

Deep learning has achieved unprecedented success in a wide range of empirical applications (Hinton et al., 2012; Luong et al., 2015; Goodfellow et al., 2016; He et al., 2016; Krizhevsky et al., 2017). Simple optimization methods such as stochastic gradient descent (SGD) (Bottou, 1999; Sutskever et al., 2013; Mori and Ueda, 2020a) and its variants (Duchi et al., 2011; Flammarion and Bach, 2015; Kingma and Ba, 2017) are often used to minimize the training error. In an overparametrized regime, a network trained by SGD shows impressive generalization performance (Zhang et al., 2017). Despite the empirical power and efficiency of SGD, our theoretical understanding of SGD is still limited. So far, nearly all the theoretical attempts at understanding SGD have adopted the continuous-time approximation by assuming vanishingly small learning rate (Mandt et al., 2017; Li et al., 2017; Jastrzebski et al., 2018; Chaudhari and Soatto, 2018; Zhu et al., 2019; Xie et al., 2020). In this regime, two types of noises are studied. When the noise is white, the governing dynamics is approximated by the Stochastic Gradient Langevin Dynamics (SGLD) (Welling and Teh, 2011). When the noise is due to mini-batch sampling, the noise is often called the SGD noise or mini-batch noise. This amounts to establishing an analogy with the continuous diffusion theory in physics (Einstein, 2005; Van Kampen, 2011), and has helped quantitatively understand some properties and phenomena of SGD and deep learning such as the flatness of the minima selected by training (Jastrzebski et al., 2018; Chaudhari and Soatto, 2018; Smith and Le, 2017; Xie et al., 2020). However, in reality a large learning rate often leads to qualitatively distinct behavior, including reduced training time and better generalization performance (Shirish Keskar et al., 2016; Li et al., 2019). The primary motivation of this work is that the existing continuous theory is insufficient to describe and predict the properties and phenomena in this large learning rate regime. The prediction may deviate arbitrarily from the experimental result.

In this work, we aim at providing exact steady-state solutions of the original discrete-time update rules of SGD and its variants with momentum, which can be utilized to exactly analyze SGD without invoking the unrealistic assumption of vanishingly small learning rate. Specifically, our contributions are:

*Corresponding authors.

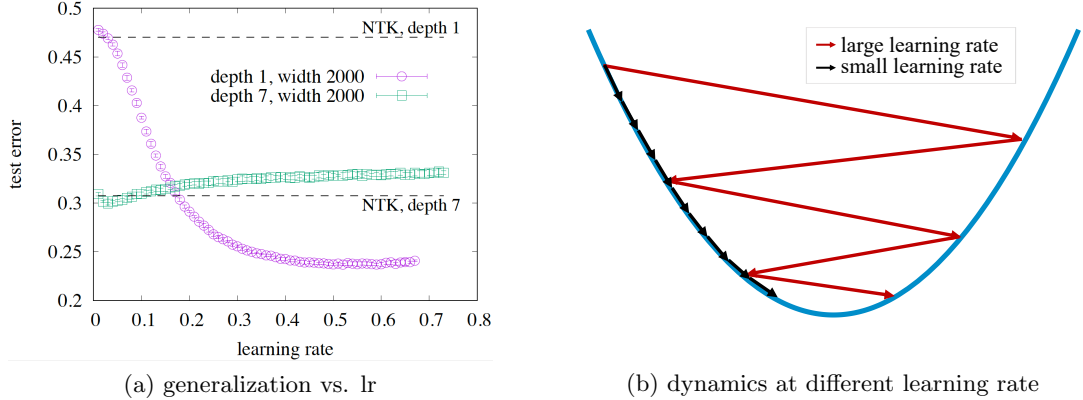


Figure 1: (a) Learning rate dependence of the generalization performance. Nonlinear feedforward neural networks of different depths are trained on a simple task with varying learning rates. We see that, when the learning rate is vanishingly small so that the continuous-time approximation is good, the continuous neural tangent kernel (NTK) provides an accurate characterization of the result of training. However, as the learning rate becomes large, the learning deviates significantly and qualitatively from the NTK prediction, sometimes for the good, sometimes for the bad. Reproduced from [Mori and Ueda \(2020b\)](#). For other interesting large learning rate related experiments, see [Lewkowycz et al. \(2020\)](#). (b) Schematic illustrations of the deterministic continuous-time evolution given by $w = w_0 e^{-\lambda kt}$ for small λ and the deterministic discrete-time evolution given by Eq. (2) for $1/k < \lambda < 2/k$. The black arrows represent each update according to the continuous-time update rule while the red ones represent the discrete-time updates.

- When the noise is an arbitrary time-independent noise, we exactly solve the discrete-time update rules of SGD and its variants with momentum close to a local minimum to obtain the analytical form of the covariance matrix of the model parameters in the asymptotic time.
- The steady-state distributions of model parameters can be analytically obtained when the noise is Gaussian.
- We apply our results to various settings that have been studied in the continuous-time limit, such as finding the optimal learning rate in a Bayesian setting, understanding the escape from a sharp minimum and the approximation error of various variants of SGD.
- Compared with the continuous-time theories, our work requires fewer assumptions and finds significantly improved agreement with experimental results.

In section 2 we state the background of this work and briefly review the continuous-time theory and some of its results. Related works are discussed in section 3. In section 4, we derive our main theoretical results, namely the steady distributions and the approximation error, for a constant SGD and its momentum variant. In section 5, we present the results of our experiments on the stable distributions with white or mini-batch noise in one- and two-dimensional models to confirm our theoretical results. In section 6, we apply our solution to some well-known problems that have previously been investigated in the continuous-time limit. We also calculate the stable distributions of two more algorithms: the Natural Gradient Descent (NGD) and the Damped Newton’s Method (DNM). In the last section, we summarize our work and discuss possible future works. A summary of our results for a specific case is given in Table 1.

2 Background

Theoretically, we know almost nothing about the properties of SGD in the case of a finite learning rate. This means that pretty much of the existing theoretical results have limited relevance to empirical practices, where

the learning rate is often in the non-vanishing regime, introducing qualitative behaviors that are different from the continuous-time limit. See Figure 1(a) for an example on the generalization performance.

To intuitively understand how large learning rate makes a difference, we consider a model with a single parameter $w \in \mathbb{R}$ in a quadratic potential $L = \frac{1}{2}kw^2$ with $k > 0$. SGD obeys the dynamical equations as follows (Mandt et al., 2017):

$$\begin{cases} g_t = kw_{t-1} + \eta_{t-1} \\ w_t = w_{t-1} - \lambda g_t. \end{cases} \quad (1)$$

where λ is the learning rate and η is a normal random variable with zero mean and variance σ^2 . When $\sigma^2 = 0$, the dynamics is deterministic, and the common approach is to assume that $\lambda \ll 1/k$ such that one may take the continuous-time limit of this equation as $\dot{w} = -\lambda kw(t)$, which solves to give $w = w_0 e^{-\lambda kt}$. However, this continuous approximation fails when λ is large. To see this, we note that the deterministic discrete-time dynamics solves to give

$$w_t = (1 - \lambda k)^t w_0, \text{ for } t \in \mathbb{N}^0, \quad (2)$$

which is an exponential decay when $\lambda < \frac{1}{k}$, and, in this region, the standard continuous time dynamics is valid and the error is $O((1 - \lambda k)^2)$. See a schematic illustration in Figure 1(b). On the other hand, when $\lambda > \frac{2}{k}$, the learning is so large that the parameter w will diverge; therefore, the interesting region is when $\frac{1}{k} < \lambda < \frac{2}{k}$, where the dynamics is convergent, yet a simple continuous-time approximation fails.

In the presence of noise, it is difficult to give a simple solution to the dynamics. Under the assumptions of constant Gaussian noise, a quadratic loss function and an infinitesimal learning rate, theorists approximate the multidimensional updating rule by a continuous-time stochastic differential equation (Mandt et al., 2017; Zhu et al., 2019):

$$dw_t = -\lambda K w_t dt + \lambda C^{\frac{1}{2}} dW_t, \quad (3)$$

where C is the covariance matrix of the noise, W_t represents a standard multidimensional Brownian motion, and K is the Hessian of the local minimum. The continuous dynamics (3) is the multivariate Ornstein-Uhlenbeck process. The covariance matrix of its steady distribution is found to satisfy the following matrix equation (Van Kampen, 2011):

$$\Sigma K + K \Sigma = \frac{\lambda}{1 - \mu} C. \quad (4)$$

where μ is the momentum hyperparameter; when no momentum is used, $\mu = 0$. This matrix equation can be regarded as an example of the fluctuation-dissipation theorem in physics (Einstein, 2005; Kubo, 1966; Funo et al., 2018), which relates the covariance (fluctuation) of the variables under consideration to the strength of the random noises (dissipation) in the system.

Despite the fact that a number of theoretical works has been done on the basis of the above continuous-time approximation (Chaudhari and Soatto, 2018; Jacot et al., 2018; Zhu et al., 2019; Lee et al., 2019; Xie et al., 2020), it is clear that the steady distribution given by Eq. (4) substantially deviates from the true one obtained by experiments¹. The predictions based on these results are qualitatively acceptable only in a small learning rate regime. For a large learning rate, the assumptions simply break down so that the theory becomes invalid. In practice, a larger learning rate usually generalizes better (Goyal et al., 2017; Hoffer et al., 2017; Li et al., 2019). One possible mechanism is that a larger learning rate leads to a flatter minimum with a smaller curvature, which exhibits better generalization performance due to the robustness against parameter perturbations (Shirish Keskar et al., 2016; Jiang* et al., 2020). It is therefore urgent to develop a theory that can handle SGD with a large learning rate. The results of this work are summarized in Table 1.

¹For example, Figure 1 in Mandt et al. (2017) plots the stationary distributions obtained from stochastic differential equations. It can be seen that these distributions generally deviate from experiments. In Gitman et al. (2019), predictions also deviate far from experiments when the learning rate is large.

Table 1: Summary of the results of this work and comparison with previous results. For notational conciseness, we only show the results when the noise matrix C commutes with the Hessian K for Σ . For the *approximation error* panel, the results apply to any positive-definite K and C . The previous Σ 's for SGD and SGDM are taken from Mandt et al. (2017), and the other four previous results are due to Gitman et al. (2019). There is no existing continuous-time result about DNM and NGD.

	Previous Work	This Work
	Σ	Σ
SGD	$\frac{\lambda}{2}K^{-1}C$	$\lambda[K(2I_D - \lambda K)]^{-1}C$
SGDM	$\frac{\lambda}{2(1-\mu)}K^{-1}C$	$\lambda\left[\frac{K}{1+\mu}\left(2I_D - \frac{\lambda K}{1+\mu}\right)\right]^{-1}\frac{C}{1-\mu^2}$
QHM	$\frac{\lambda}{2(1-\mu)}K^{-1}C + O(\lambda^2)$	$\lambda^2 h(K)^{-1}C$ [Eq. (57)]
DNM	-	$\frac{1+\mu}{1-\mu}\frac{\lambda}{2(1+\mu)-\lambda}K^{-2}C$
NGD	-	$\frac{1}{2}K^{-1}\left[Q + \frac{\lambda}{2(1+\mu)}I_D\right]$ [Eq. (62)]
	Approximation Error	Approximation Error
SGD	$\frac{\lambda}{4}\text{Tr}[C] + \frac{\lambda^2}{8}\text{Tr}[KC] + O(\lambda^3)$	$\frac{\lambda}{2}\text{Tr}[(2I_D - \lambda K)^{-1}C]$
SGDM	$\frac{\lambda}{4(1-\mu)}\text{Tr}[C] + \frac{\lambda^2}{8}\frac{1}{1-\mu^2}\text{Tr}[KC] + O(\lambda^3)$	$\frac{\lambda}{2(1-\mu)}\text{Tr}\left[\left(2I_D - \frac{\lambda}{1+\mu}K\right)^{-1}C\right]$
QHM	$\frac{\lambda}{4}\text{Tr}[C] + \frac{\lambda^2}{8}\left[1 + \frac{2\mu\nu}{1-\mu}\left(\frac{2\mu\nu}{1+\mu} - 1\right)\right]\text{Tr}[KC] + O(\lambda^3)$	$\frac{\lambda^2}{2}\text{Tr}[h(K)^{-1}KC]$ [Eq. (56)]
DNM	-	$\frac{1+\mu}{1-\mu}\frac{\lambda}{4(1+\mu)-2\lambda}\text{Tr}(K^{-1}C)$
NGD	-	$\frac{1}{4}\text{Tr}\left[Q + \frac{\lambda}{2(1+\mu)}I_D\right]$

*SGD: stochastic gradient descent with learning rate λ . *SGDM: stochastic gradient descent with momentum hyperparameter μ .

*QHM: quasi-hyperbolic momentum. *DNM: damped newton's method. *NGD: natural gradient descent.

3 Related Works

3.1 Small and Large Learning Rate

In the vanishing learning rate regime, SGD is now relatively well understood, and the majority of theoretical approaches to SGD assume the continuous-time limit. For example, when the learning rate is vanishingly small, the dynamics of the learning of a neural network is known to behave like a special kernel called neural tangent kernel when the network is infinitely wide (Jacot et al., 2018) or finitely wide (Hanin and Nica, 2019). This regime has been called the “lazy” learning regime, since global minima are known to exist very close to initialization and the model parameters do not have to move much to converge; however, it is now known that lazy learning is in general detrimental to generalization (Chizat and Bach, 2018).

Although continuous-time theory has been the dominant theoretical approach, Lewkowycz et al. (2020) took a step forward in understanding why a larger learning rate prefers a flatter minimum. They characterized SGD into three regimes according to the learning rate through comparison with the initial curvature. They conjectured that a rather large learning rate which they call a catapult phase often leads to optimal generalization by converging to a flatter minimum. However, their work is mostly empirical and in the noise-free regime.

There are more empirical works on large learning rate and generalization. LeCun et al. (2012) found that a large batch size (or a small learning rate) usually leads to reduced generalization performance. Shirish Keskar et al. (2016) proposed an empirical measure based on the sharpness or flatness of the selected minimum. They presented numerical evidence that a small learning rate tends to converge to sharp minima which generalize poorly. Goyal et al. (2017) proved that setting a learning rate proportional to the mini-batch size ensures good generalization, which is crucial for large scale training. There are also works about the roles played by the noise, batch size and learning rate influencing the generalization (Hoffer et al., 2017; Mori and Ueda, 2020a,b). These works all hint at that a large learning rate leads to flatter minima that generalize better. As

for why a flatter minimum has better generalization ability, there are some explanations and theories such as the minimum description length theory (Rissanen, 1983), a Bayesian view of learning (MacKay, 1992), and the Gibbs free energy (Chaudhari et al., 2019).

3.2 Escape Rate from a Sharp Minimum

Theoretical understanding on how SGD chooses flatter minima usually seeks help from continuous-time theories. That escape from a sharp minimum is easier than from a flat one was studied by Hu et al. (2018) using diffusion theory. Wu et al. (2018) studied the relationship among learning rate, batch size and performance from the perspective of dynamical stability. Jastrzebski et al. (2018) used stochastic differential equations to prove that the higher the ratio of the learning rate to the batch size, the flatter minimum will be selected. Zhu et al. (2019) defined the escape efficiency for a minimum and obtained its explicit expression using diffusion theory. They show that anisotropic noise helps escape from sharp minima effectively. A more recent work by Xie et al. (2020) calculated the escape rate from a minimum by adopting the formalism of the Kramers escape rate in physics (Kramers, 1940; Talkner et al., 1987). It is shown that SGD with mini-batch noise favors flatter minima.

Theoretically understanding why and how SGD converges to flat minima is important. Many different complexity measures which monotonically relate to some aspects of generalization performance have been proposed both theoretically (Vapnik and Chervonenkis, 1971; Neyshabur et al., 2017; Dziugaite and Roy, 2017; Neyshabur et al., 2018) and empirically (Smith and Le, 2017; Chaudhari and Soatto, 2018; Shirish Keskar et al., 2016; Liang et al., 2019; Nagarajan and Kolter, 2019; Wilson et al., 2017). It has been found that sharpness-based measures are the best up to now (Jiang* et al., 2020). Our exact results for large learning rate make it possible to study the flatness selected by SGD and the complexity measures more accurately. This will enhance our understanding of generalization in deep learning.

3.3 Bayesian Inference

SGD has been used as Bayesian inference as well. In Bayesian inference, we assume a probabilistic model $p(w, x)$ with data x and hidden parameter w . The goal is to approximate the posterior $p(w|x)$. Traditionally stochastic gradient Markov Chain Monte Carlo (MCMC) methods have been used (Welling and Teh, 2011; Ma et al., 2015). A similarity between SGD and MCMC suggests the possibility of SGD being used as approximate Bayesian inference (Mandt et al., 2017). Mandt et al. (2017) applied SGD to minimize the negative log probability $-\ln p(w, x)$ which serves as a loss function. By tuning the learning rate and the batch size, they found the steady distribution which is closest to the posterior by minimizing the Kullback-Leibler (KL) divergence between these two distributions. Equipped with these optimal parameters, SGD can be regarded as an approximate Bayesian inference. However, for a large learning rate, their assumption is no more valid and their theory cannot give any meaningful prediction about how to select the optimal learning rate. Our exact results provide the possibility to deal with the large learning rate regime.

4 Theory of Discrete-Time Stochastic Gradient Descent

Contrary to the often used continuous-time approximation, we propose to directly deal with the original discrete-time updating rule². We first solve the simplest case without momentum. The general result with momentum is given in Section 4.2.

Notation-wise, we use capital K to denote the Hessian matrix of the quadratic loss function. When K is one-dimensional, we write in lower-case k for clarity. we use \mathbf{w} to denote the weights of the model

²In spirit, the work that is the closest to the present work is due to Yaida (2018). However, the formalism adopted by Yaida (2018) follows the statistical physics convention, and the focus of the paper is on the derivation of the abstract relations rather than the exact and solvable results. Another work worth mentioning is Gitman et al. (2019). However, Gitman et al. (2019) focus on the effect of momentum and only solves the same problem as ours in a small learning rate regime by means of the Taylor expansion of the learning rate. Therefore, their result is only correct at small learning rate and for the momentum hyperparameter μ that is away from 1. In contrast, we derive the exact solutions that are applicable to all regimes of the learning rate and the momentum hyperparameter.

viewed as a vector. We use Σ to denote the covariance matrix of \mathbf{w} , and C denotes the covariance matrix of the time-independent noise η , which often has the same dimension as \mathbf{w} . λ denotes the learning rate, L the training loss function, S the mini-batch size. The capital T is used as a superscript denoting matrix transpose and lower case t denotes the time step of optimization; when the learning rate is not a scalar but a preconditioning matrix, we use the upper case Λ instead of λ . Other more specific notations and parameters are defined in the context.

4.1 SGD

A general form of a quadratic potential approximated from the loss function is given by

$$L(\mathbf{w}') = \frac{1}{2}(\mathbf{w}' - \mathbf{w}^*)^T K(\mathbf{w}' - \mathbf{w}^*), \quad (5)$$

where the Hessian K is a symmetric positive definite matrix, and \mathbf{w}^* is a constant vector. One can redefine $\mathbf{w}' - \mathbf{w}^* \rightarrow \mathbf{w}$ to obtain a simplified form: $L(\mathbf{w}) = \mathbf{w}^T K \mathbf{w} / 2$. The updating rule for \mathbf{w} is given by

$$\begin{aligned} \mathbf{w}_t &= \mathbf{w}_{t-1} - \lambda K \mathbf{w}_{t-1} + \lambda \eta_{t-1} \\ &= (I_D - \lambda K) [(I_D - \lambda K) \mathbf{w}_{t-2} + \lambda \eta_{t-2}] + \lambda \eta_{t-1} \\ &= (I_D - \lambda K)^t \mathbf{w}_0 + \lambda \sum_{i=0}^{t-1} (I_D - \lambda K)^i \eta_{t-1-i}, \end{aligned} \quad (6)$$

where the noise η_t is assumed to be Gaussian with a symmetric covariance $C := BB^T$ for some general matrix B . Let k^* be the largest eigenvalue of K . For any minimum with $\lambda k^* > 2$, the dynamics will not converge, and \mathbf{w} will simply escape from this minimum. Therefore, we focus on the range of $0 < \lambda < \frac{2}{k^*}$. This means that the absolute values of all the eigenvalues of $(I_D - \lambda K)$ are in the range of $[0, 1)$. Since we are interested in the steady distribution of \mathbf{w} , we take the long-time limit to obtain

$$\begin{aligned} \lim_{t \rightarrow \infty} \mathbf{w}_t &= \lim_{t \rightarrow \infty} \lambda \sum_{i=0}^{t-1} (I_D - \lambda K)^i \eta_{t-1-i} \\ &\sim \lim_{t \rightarrow \infty} \mathcal{N}\left(0, \lambda^2 \sum_{i=0}^{t-1} (I_D - \lambda K)^i C (I_D - \lambda K)^i\right) := \mathcal{N}(0, \Sigma), \end{aligned} \quad (7)$$

where we define Σ to be the covariance matrix of \mathbf{w} at a stationary state. After some mathematical manipulation, we find that the covariance matrix satisfies the matrix equation³

$$\Sigma K + K \Sigma - \lambda K \Sigma K = \lambda C, \quad (8)$$

This equation is solvable (Xu et al., 1998), although a simple analytical solution is not known to exist. It is best to keep the above simple matrix equation form. Thus, we have derived the following result.

Theorem 1. (Stable distribution of discrete SGD in a quadratic potential.) *Let \mathbf{w}_t evolve according to (6), where η_t is sampled from a zero-mean multivariate gaussian distribution with $\eta_t^T \eta_{t'} = \delta_{t,t'} C$, and $C = a(\lambda) B B^T$. Then the steady state distribution of \mathbf{w} is given by*

$$\mathbf{w} \sim \mathcal{N}(0, \Sigma), \quad (9)$$

where Σ satisfies $\Sigma K + K \Sigma - \lambda K \Sigma K = \lambda C$.

Remark. *The exact condition $\lambda \Sigma K + \lambda K \Sigma - \lambda^2 K \Sigma K = \lambda^2 C$ is different from the classical result obtained for a continuous-time Ornstein-Uhlenbeck process, which has $\lambda \Sigma K + \lambda K \Sigma = \lambda^2 C$. This suggests that, the approximation of a discrete-time dynamics with a continuous-time one in Mandt et al. (2017) can be thought of as a λ -first-order approximation of the true dynamics. This approximation incurs an error of order $\mathcal{O}(\lambda^2)$. The error becomes significant or even dominant as λ gets large.*

We can derive the stable distribution explicitly when C commutes with K . In this case, the following corollary applies.

Corollary 1. *Let $[C, K] := CK - KC = 0$, then $\Sigma = \lambda [K(2I_D - \lambda K)]^{-1} C$.*

³We omit the details here since it can also be reduced from the more general result that we will derive in Section 4.2.

4.2 SGD with Momentum

In this section, we deal with SGD with momentum. When momentum is present, the update rule takes the form

$$\begin{cases} \mathbf{g}_t = K\mathbf{w}_{t-1} + \eta_{t-1}; \\ \mathbf{m}_t = \mu\mathbf{m}_{t-1} + \mathbf{g}_t; \\ \mathbf{w}_t = \mathbf{w}_{t-1} - \lambda\mathbf{m}_t. \end{cases} \quad (10)$$

In principle, the stable distribution can be found by expanding the sum, but this involves summing over too many variables. Here we take a different approach to find its stable distribution. We first assume that the stable distributions of both \mathbf{m} and \mathbf{w} exist and $\mathbb{E}[\mathbf{w}\mathbf{w}^\top] := \Sigma$. Our goal is to find Σ . We assume that \mathbf{w}_0 and \mathbf{m}_0 are sampled from the stable distribution. This is valid as long as we only try to find the asymptotic behavior of \mathbf{w}_t . By definition we have

$$\begin{aligned} \mathbb{E}[\mathbf{w}_t\mathbf{w}_t^\top] &= \mathbb{E}[(\mathbf{w}_{t-1} - \lambda\mu\mathbf{m}_{t-1} - \lambda K\mathbf{w}_{t-1} - \lambda\eta_{t-1})(\mathbf{w}_{t-1} - \lambda\mu\mathbf{m}_{t-1} - \lambda K\mathbf{w}_{t-1} - \lambda\eta_{t-1})^\top] \\ &= \mathbb{E}[(1 - \lambda K)\mathbf{w}_{t-1}\mathbf{w}_{t-1}^\top(1 - \lambda K)] + \lambda^2\mu^2\mathbb{E}[\mathbf{m}_{t-1}\mathbf{m}_{t-1}^\top] + \lambda^2 C - \mathbb{E}[A + A^\top], \end{aligned} \quad (11)$$

where $A := \lambda\mu(1 - \lambda K)\mathbf{w}_{t-1}\mathbf{m}_{t-1}^\top$. Notice that \mathbf{w}_0 is initialized according to the stable distribution, and therefore, the distribution does not depend on t , namely $\mathbb{E}[\mathbf{w}_t\mathbf{w}_t^\top] = \mathbb{E}[\mathbf{w}_{t-1}\mathbf{w}_{t-1}^\top]$. For $\mathbb{E}[\mathbf{m}_{t-1}\mathbf{m}_{t-1}^\top]$, similarly we have by definition

$$\begin{aligned} \lambda^2\mathbb{E}[\mathbf{m}_{t-1}\mathbf{m}_{t-1}^\top] &= \mathbb{E}[(\mathbf{w}_{t-1} - \mathbf{w}_{t-2})(\mathbf{w}_{t-1} - \mathbf{w}_{t-2})^\top] \\ &= 2\Sigma - \mathbb{E}[\mathbf{w}_{t-1}\mathbf{w}_{t-2}^\top] - \mathbb{E}[\mathbf{w}_{t-2}\mathbf{w}_{t-1}^\top]. \end{aligned} \quad (12)$$

For $\mathbb{E}[A + A^\top]$, we have

$$\begin{aligned} \mathbb{E}[A] &= \mathbb{E}[\lambda\mu(1 - \lambda K)\mathbf{w}_{t-1}\mathbf{m}_{t-1}^\top] \\ &= \mu(1 - \lambda K)\mathbb{E}[\mathbf{w}_{t-1}(\mathbf{w}_{t-2} - \mathbf{w}_{t-1})^\top] \\ &= -\mu(1 - \lambda K)\Sigma + \mu(1 - \lambda K)\mathbb{E}[\mathbf{w}_{t-1}\mathbf{w}_{t-2}^\top]. \end{aligned} \quad (13)$$

Therefore, we are left to solve for $\mathbb{E}[\mathbf{w}_{t-1}\mathbf{w}_{t-2}^\top]$. Using the fact of stationary state that the expectations are time-independent, we obtain

$$\begin{aligned} \mathbb{E}[\mathbf{w}_{t-1}\mathbf{w}_{t-2}^\top] &= \mathbb{E}[\mathbf{w}_t\mathbf{w}_{t-1}^\top] = \mathbb{E}[(\mathbf{w}_{t-1} - \lambda\mu\mathbf{m}_{t-1} - \lambda K\mathbf{w}_{t-1} - \lambda\eta_{t-1})\mathbf{w}_{t-1}^\top] \\ &= (1 - \lambda K)\Sigma - \mathbb{E}[\lambda\mu\mathbf{m}_{t-1}\mathbf{w}_{t-1}^\top] \\ &= (1 - \lambda K)\Sigma + \mu\Sigma - \mu\mathbb{E}[\mathbf{w}_{t-2}\mathbf{w}_{t-1}^\top]. \end{aligned} \quad (14)$$

Taking transposition yields

$$\mathbb{E}[\mathbf{w}_{t-2}\mathbf{w}_{t-1}^\top] = \Sigma(1 - \lambda K) + \mu\Sigma - \mu\mathbb{E}[\mathbf{w}_{t-1}\mathbf{w}_{t-2}^\top]. \quad (15)$$

From the above two equations we can solve for $\mathbb{E}[\mathbf{w}_{t-1}\mathbf{w}_{t-2}^\top]$ and $\mathbb{E}[\mathbf{w}_{t-2}\mathbf{w}_{t-1}^\top]$, respectively.

Finally, we are ready to plug everything back into (11) to obtain

$$\underbrace{(1 - \mu)\lambda(K\Sigma + \Sigma K)}_{\text{continuous-time}} - \underbrace{\frac{1 + \mu^2}{1 - \mu^2}\lambda^2 K\Sigma K + \frac{\mu}{1 - \mu^2}\lambda^2(K^2\Sigma + \Sigma K^2)}_{\text{discrete-time}} = \lambda^2 C. \quad (16)$$

This result can also be equivalently rewritten in the form of commutators as

$$\underbrace{(1 - \mu)\lambda K \left(2I_D - \frac{\lambda}{1 + \mu} K \right) \Sigma}_{\text{commuting contribution}} + \underbrace{(1 - \mu)\lambda \left(I_D - \frac{\lambda}{1 + \mu} K \right) [\Sigma, K] + \frac{\mu}{1 - \mu^2}\lambda^2 [K, [K, \Sigma]]}_{\text{non-commuting contribution}} = \lambda^2 C, \quad (17)$$

and the non-commuting contribution is caused by C and K that do not commute with each other. Otherwise, when $[C, K] = 0$, we have $[\Sigma, K] = 0$ so that the non-commuting term vanishes.

We examine the above result (16) with two limiting examples. First, if there is no momentum, namely $\mu = 0$, we simply recover our previous result (8) without momentum. Next, if $\lambda K \ll 1$, we recover the result of continuous-time approximation with momentum (4) derived by Mandt et al. (2017) by neglecting the $\mathcal{O}((\lambda K)^2)$ terms.

When the noise C commutes with K , we can solve the above equation explicitly as

$$\begin{aligned}\Sigma &= \left[\frac{\lambda K}{1 + \mu} \left(2I_D - \frac{\lambda K}{1 + \mu} \right) \right]^{-1} \frac{\lambda^2 C}{1 - \mu^2} \\ &:= [\tilde{\lambda} K (2I_D - \tilde{\lambda} K)]^{-1} \tilde{C},\end{aligned}\tag{18}$$

where we introduce the rescaling

$$\tilde{\lambda} := \frac{\lambda}{1 + \mu}, \quad \tilde{C} := \frac{1 + \mu}{1 - \mu} C.\tag{19}$$

We notice that with this rescaling and under $[C, K] = 0$, the form of the matrix equation satisfied by Σ is invariant

$$\tilde{\lambda}(K\Sigma + \Sigma K) - \tilde{\lambda}^2 K\Sigma K = \tilde{\lambda}^2 \tilde{C}.\tag{20}$$

This suggests that the learning rate can be $1 + \mu$ times larger. This general result is summarized in the following theorem.

Theorem 2. (*Stable distribution of discrete SGD with momentum.*) Let \mathbf{w}_t evolve according to (10), where η_t is sampled from a zero-mean multivariate distribution with $\eta_t^\top \eta_t = \delta_{t,v} C$ and $C = a(\lambda) B B^\top$. Then Σ is given by the solution of Eq. (16) or (17). When the noise is Gaussian, then the steady state distribution of \mathbf{w} is given by

$$\mathbf{w} \sim \mathcal{N}(0, \Sigma).\tag{21}$$

Similarly, we can solve for Σ explicitly when $[C, K] = 0$. Before giving the explicit expression, we present a lemma about the commutation relations.

Lemma 1. $[C, K] = 0$ is equivalent to $[\Sigma, K] = 0$.

The proof is given in Appendix A. With this lemma, the following corollary results.

Corollary 2. Let $[C, K] = 0$, then $\Sigma = \left[\frac{\lambda K}{1 + \mu} \left(2I_D - \frac{\lambda K}{1 + \mu} \right) \right]^{-1} \frac{\lambda^2 C}{1 - \mu^2}$.

Corollary 3. If the scalar λ is replaced by a symmetric positive-definite preconditioning matrix Λ which does not necessarily commute with the Hessian K , our theory applies as well and the matrix equation reads

$$(1 - \mu)(\Lambda K \Sigma + \Sigma K \Lambda) - \frac{1 + \mu^2}{1 - \mu^2} \Lambda K \Sigma K \Lambda + \frac{\mu}{1 - \mu^2} (\Lambda K \Lambda K \Sigma + \Sigma K \Lambda K \Lambda) = \Lambda C \Lambda.\tag{22}$$

4.3 Two Typical Kinds of Noise

To be more specific, there are two types of noise worth studying for machine learning practices. The first is a multi-dimensional white noise: $\eta \sim \mathcal{N}(0, \sigma^2 I_D)$, where σ^2 is a positive scalar. The second type of noise covariance is proportional to the Hessian, which is approximately equal to the noise caused by a mini-batch gradient descent algorithm (Hoffer et al., 2017; Zhu et al., 2019; Xie et al., 2020): $C = aK$, where a is a constant scalar. This is because the noise covariance can be expressed as

$$\begin{aligned}C(\mathbf{w}) &= \frac{1}{S} \left[\frac{1}{N} \sum_{n=1}^N \nabla L(\mathbf{w}, x_n) \nabla L(\mathbf{w}, x_n)^\top - \nabla L(\mathbf{w}) \nabla L(\mathbf{w}^\top) \right] \\ &\approx \frac{1}{S} \frac{1}{N} \sum_{n=1}^N \nabla L(\mathbf{w}, x_n) \nabla L(\mathbf{w}, x_n)^\top := \frac{1}{S} J(\mathbf{w}) \approx \frac{1}{S} K,\end{aligned}\tag{23}$$

where the first approximation is due to the fact that noise dominates the dynamics in the vicinity of a minimum and the second approximation is according to the similarity between the Fisher information $J(\mathbf{w})$ and the Hessian K near a minimum. This approximation is somewhat crude although it is well-known.

To be more general, one might want to mix an isotropic Gaussian noise with the mini-batch noise. In this case, $C = \sigma^2 I_D + aK$, and the distribution is given by the following theorem.

Theorem 3. *Let $C = \sigma^2 I_D + a(\lambda)K$. Then the stable distribution of \mathbf{w} is given by*

$$\mathcal{N}\left(0, \lambda(\sigma^2 I_D + aK)[K(2I_D - \lambda K)]^{-1}\right). \quad (24)$$

Notice that, in this case, C commutes with K . From this result, we can derive the two special cases by setting $\sigma^2 = 0$ or $a = 0$ respectively.

Corollary 4. *Let $\sigma^2 = 0$, then $\mathbf{w} \sim \mathcal{N}\left(0, a\lambda(2I_D - \lambda K)^{-1}\right)$.*

Corollary 5. *Let $a = 0$, then $\mathbf{w} \sim \mathcal{N}\left(0, \sigma^2\lambda[K(2I_D - \lambda K)]^{-1}\right)$.*

4.4 Approximation Error of SGD

We note that one important quantity for measuring the approximation error of SGD is the $\text{Tr}[K\Sigma]$, since, for a quadratic loss of the form $\mathbf{w}^T K \mathbf{w}/2$, we have

$$\mathbb{E}\left[\frac{1}{2}\mathbf{w}^T K \mathbf{w}\right] = \frac{1}{2}\text{Tr}[K\Sigma], \quad (25)$$

where the expectation is taken over the stable distribution of \mathbf{w} . This means that $\frac{1}{2}\text{Tr}[K\Sigma]$ is the expected training loss.

In the presence of momentum, we start from Eq. (17), and multiply by $S := \left(2I_D - \frac{\lambda}{1+\mu}K\right)^{-1}$ from the left to obtain a function of the form

$$(1 - \mu)\text{Tr}[K\Sigma] + \text{Tr}[SA_1] + \text{Tr}[SA_2] = \lambda^2\text{Tr}\left[\left(2I_D - \frac{\lambda}{1+\mu}K\right)^{-1} C\right], \quad (26)$$

where A_1 and A_2 are the matrices resulting from the commutators of the form $[K, \Sigma]$ etc., which are anti-symmetric by definition. Because S is symmetric by definition, the traces $\text{Tr}[SA_1]$ and $\text{Tr}[SA_2]$ therefore vanish. This means that for general noise covariance C and Hessian K , the approximation error for SGD with momentum is

$$\frac{1}{2}\text{Tr}[K\Sigma] = \frac{\lambda}{4(1-\mu)}\text{Tr}\left[\left(I_D - \frac{\lambda}{2(1+\mu)}K\right)^{-1} C\right]. \quad (27)$$

This can be compared with the result for continuous-time dynamics: $\frac{1}{2}\text{Tr}[K\Sigma] = \frac{\lambda}{4(1-\mu)}\text{Tr}C$, which shows that the discrete-time dynamics results in a larger approximation error (i.e., training error) and the approximation error is larger for the direction with a larger eigenvalue in the Hessian.

4.5 Necessary Stability Condition

The main result in Theorem 2 also suggests a condition for the convergence of SGD with momentum. In order for a stable distribution to exist at convergence, the covariance Σ needs to exist and be positive-definite, and this is only possible when $\left(2I_D - \frac{\lambda}{1+\mu}K\right)$ is positive-definite. This condition may be called the *ill-conditioning problem of discrete-time SGD*, which means that, when λ is large, the optimization problem becomes increasingly ill-conditioned, and the necessary condition is that $\left(2I_D - \frac{\lambda}{1+\mu}K\right)$ is positive-definite. Since this condition is only asymptotic, it is may not be sufficient in order to guarantee convergence. One more implication of this is that using momentum may mitigate the ill-conditioning problem of the large learning rate, but only up to a factor of $1 + \mu < 2$, before the momentum causes another divergence problem due to the term $\frac{1}{1-\mu}$. Therefore, when momentum is used, the necessary condition for convergence becomes $\lambda k^* \leq 2(1 + \mu) < 4$.

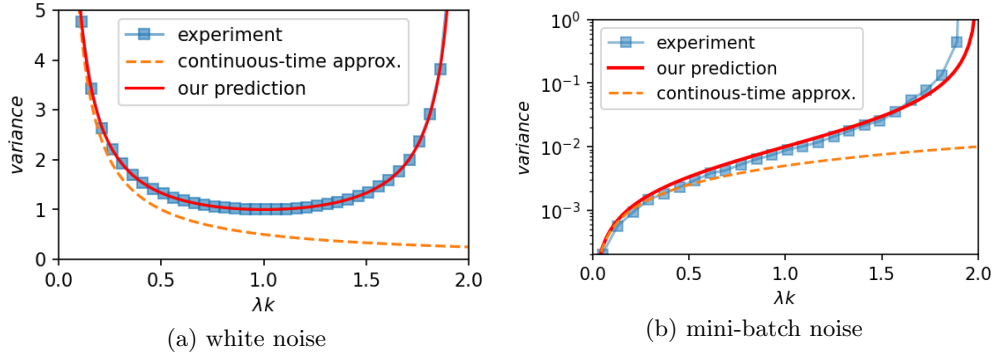


Figure 2: Comparison for a 1-dimensional example for the prediction of Σ . We see that the continuous-time prediction is only acceptable for $\lambda k < 1$, while the discrete-time theory holds well for all non-diverging learning rates. (a) White noise with strength $\sigma^2 = 1$. (b) Mini-batch noise.

5 Experiments

In this section, we perform experiments to confirm our theory. We start with an isotropic Gaussian noise, and then investigate the mini-batch noise. We test the general case when the momentum is present as well.

5.1 Isotropic Gaussian Noise

We first consider the case when $w \in \mathbb{R}$ is one-dimensional. Let the loss function be $L(w) = \frac{1}{2}kw^2$ with $k = 1$. In Figure 2(a), we plot the variance of the variable w after 1000 training steps. We compare the prediction of our model from Corollary 1 with that of the continuous-time approximation used by Mandt et al. (2017). We see that our theory agrees with experiment exactly, while the standard continuous-time approximation fails as λ increases. Moreover, the continuous-time approximation fails to predict the divergence of the variance at $\lambda k \rightarrow 2$ while our theory captures this exactly.

Now, we consider a multidimensional case. We set the loss function to be

$$L(\mathbf{w}) = \frac{1}{2} \mathbf{w}^T K \mathbf{w}$$

For visualization, we choose $D = 2$, and we set the eigenvalues of the Hessian matrix to be 1 and 0.1, and plot the fluctuation along the eigenvectors of this Hessian matrix. See Figure 3. As before, we compare with the theoretical predictions of Mandt et al. (2017). After diagonalization, the continuous-time dynamics predicts $\Sigma = \text{diag}(\lambda/2, \lambda/0.2)$, whereas our theory predicts $\Sigma = \text{diag}\left(\frac{\lambda}{2-\lambda}, \frac{\lambda}{0.1(2-0.1\lambda)}\right)$. We find that our theory finds a much better overall agreement with the experiment and successfully predicts a distortion along the direction with large eigenvalue in the Hessian. This suggests that continuous-time approximation always underestimates the fluctuation in the learning and the discrepancy is larger as the learning rate gets larger; the prediction of the continuous-time theory can become arbitrarily far from the experiment as λ gets close to the divergence value.

5.2 Mini-Batch Noise

For mini-batch noise, we let the task be a linear regression task with the loss function

$$L(w) = \frac{1}{N} \sum_i^N (\mathbf{w}^T x_i - y_i)^2, \quad (28)$$

where $N = 1000$ is the number of data points, data x_i are sampled independently from a normal distribution $\mathcal{N}(0, 1)$; $y_i = \mathbf{w}^* x_i + \epsilon_i$ with a constant but fixed \mathbf{w}^* and ϵ_i are also sampled from a normal distribution. For sampling of mini-batches, we use sampling with replacement with $S = 100$. As before, we first compare

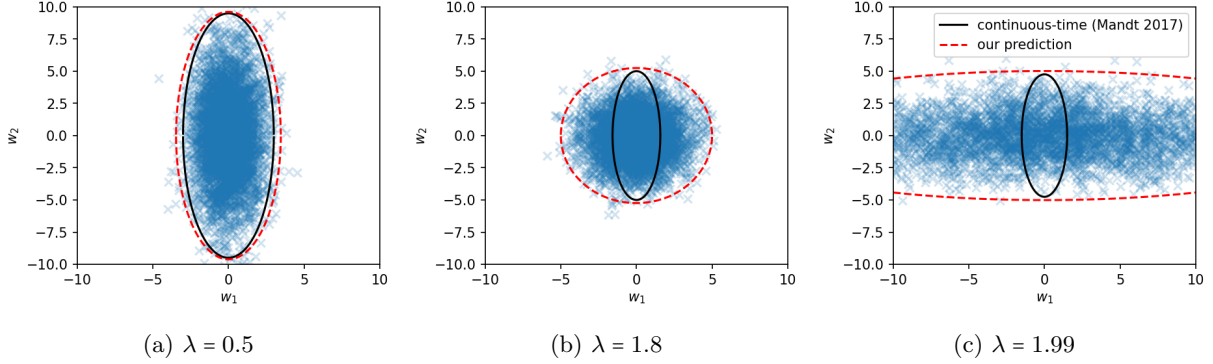


Figure 3: Comparison between our prediction and that of Mandt et al. (2017) for white noise at the predicted 3σ confidence interval, i.e., 99% of data points lie within the boundary of the theory. We see that our prediction agrees well with the experimental distribution across all levels of the learning rate, whereas the prediction by Mandt et al. (2017) only applies when λ is small, as is required by their continuous-time approximation.

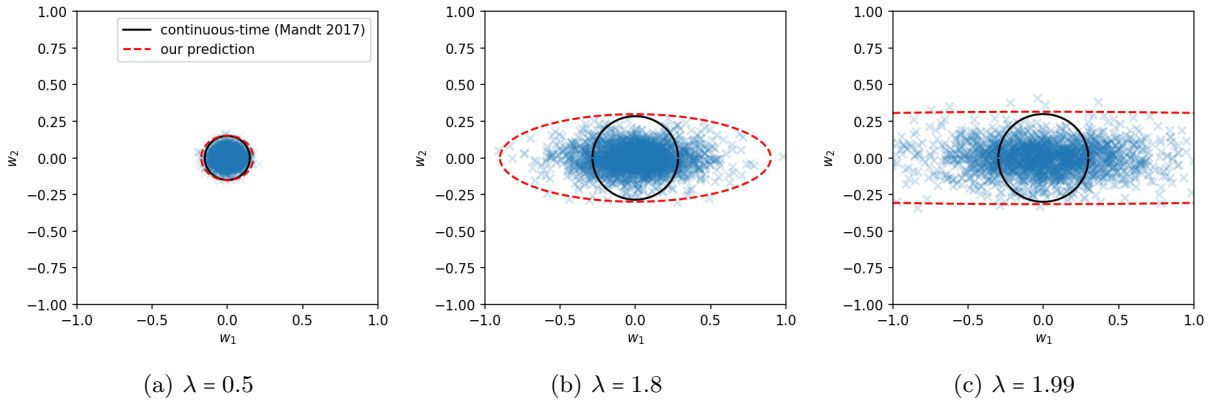


Figure 4: Comparison between our prediction and that by Mandt et al. (2017) at the predicted 3σ confidence interval for mini-batch noise. We see that our prediction agrees well with the experimental distribution across all levels of the learning rate, whereas that by Mandt et al. (2017) only applies when λ is small as well.

the predicted variance of w for a one-dimensional problem, and then compare the predicted distribution on a two-dimensional problem. As discussed in the main text, the theoretical noise covariance matrix C is approximated with $C \approx K/S$. See Figure 2(b) for the 1d comparison. We see that, the proposed theory agrees much better with experiment than the continuous-time theory, both in trend and in magnitude. We also compare the predicted distribution when $D = 2$. Here, the data points x_i are sampled from $\mathcal{N}(0, \text{diag}(1, 0.1))$, which makes the expected Hessian equal to $\text{diag}(1, 0.1)$. See Figure 4 for the illustration. Again, an overall agreement with experiment is much better for the proposed theory. We notice that the prediction by Mandt et al. (2017) and our theory agree well with each other when λ is small, suggesting that in the continuous-time limit, the mini-batch noise causes an isotropic fluctuation in the learned parameters. Interestingly, our theory slightly over-estimates the variance of the parameters. This suggests the limitation of the commonly used approximation of the mini-batch noise $C \sim H(w)$. It is, in fact, interesting and important to study the mini-batch noise in our setting in a rigorous way. We leave this to a future work.

5.3 SGD with Momentum

For white noise, we set $L(w) = w^T x w / 2$ as before. In Figure 5(a), we plot the case with $\lambda k > 2$. This is the case where the dynamics will diverge if no momentum is present. The experiment does show the divergence at the value of $\mu \rightarrow \lambda k / 2 - 1$ predicted by our theory, in contrast to the continuous-time theory that predicts no divergence. In Figure 5(b), we plot the case with $\lambda k = 1$; this is the case in which there is no divergence

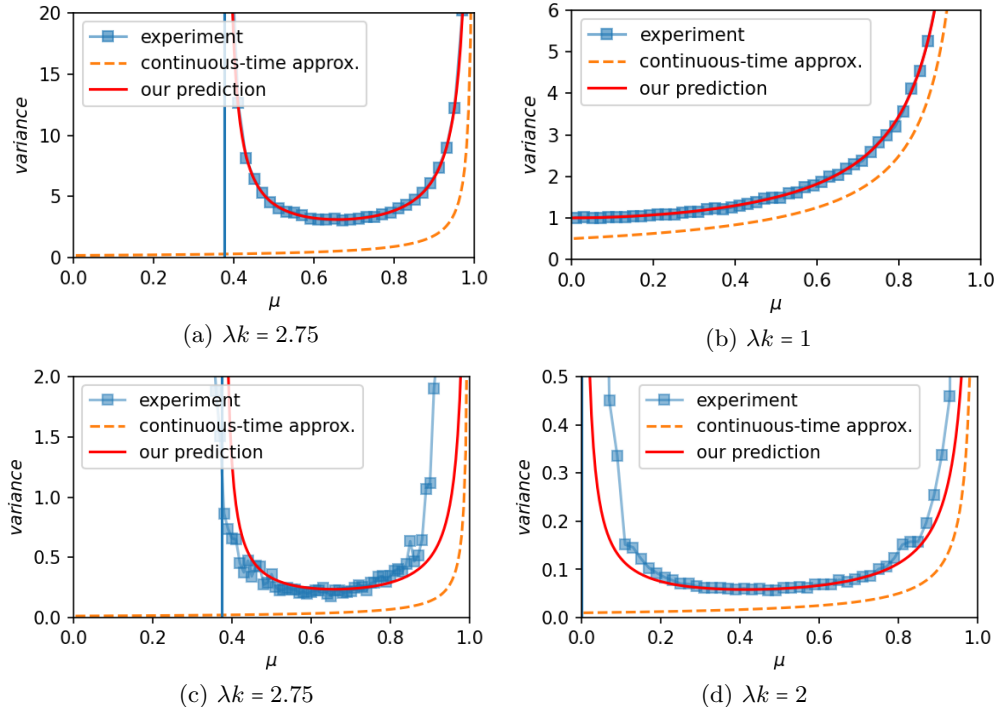


Figure 5: Comparison between continuous-time theory and our discrete-time theory when momentum is present. (a)-(b) White noise. (c)-(d) Mini-batch noise. (a) $\lambda k = 2.75$. The vertical line shows $\mu = \frac{\lambda k - 2}{2}$, where the variance is predicted to diverge. (b) $\lambda k = 1$. In this case, the fluctuation does not diverge when $\mu < 1$. However, the error of the continuous-time approximation does not diminish even if μ gets large. (c)-(d) Even in the case of mini-batch noise, the proposed theory agrees much better with the experiments.

for $\mu < 1$. Here, we see that the continuous-time theory predicts with an error that does not diminish even if μ is close to 1. In Figure 5(c)-(d), we show the experiments with mini-batch noise. The task is exactly the same as the previous section. The predicted theory agrees better than the continuous-time approximation. On the other hand, the agreement becomes worse as the fluctuation in w becomes large. This suggests the limitation⁴ of the commonly used approximation of mini-batch noise, i.e., $C \sim H(w) = K$.

6 Applications

In this section, we apply our exact solution to some well-known problems, such as derivation of the Bayesian optimal learning rate in Section 6.1, and escape from a sharp minimum⁵ in Sections 6.2 and 6.3. Previously, these problems have been solved with the continuous-time approximation. Therefore the results incur an error of order $(\lambda K)^2$, and this error may become arbitrarily large when $\lambda k^* = \mathcal{O}(1)$. It is therefore of interest to investigate how our exact solution corrects the established results in the large- λ regime.

⁴We note that a slightly better approximation is $C = K\Sigma K$; see the discussion in Section 6.5.

⁵In the existing machine learning literature, there are two definitions for the escape rate. The first was introduced by Zhu et al. (2019). We call it the “escape rate of the first kind” (in theoretical physics, this rate should more properly be called the “thermalization rate” rather than the “escape rate”). The second type is the familiar “Kramers escape rate” (Kramers, 1940; Van Kampen, 2011), which, in a machine-learning context, was first dealt with by Xie et al. (2020).

6.1 Optimal Bayesian Learning Rate

We use SGD as an approximate Bayesian inference algorithm. We assume a probabilistic model $p(\mathbf{w}, \mathbf{x})$ with N -dimensional data \mathbf{x} . Our goal is to approximate the posterior

$$p(\mathbf{w}|\mathbf{x}) = \exp[\ln p(\mathbf{w}, \mathbf{x}) - \ln p(\mathbf{x})]. \quad (29)$$

The loss function is defined as

$$L(\mathbf{w}) := \frac{1}{N} \sum_{n=1}^N l_n(\mathbf{w}), \quad (30)$$

where

$$l_n(\mathbf{w}) := -\ln p(x_n|\mathbf{w}) - \frac{1}{N} \ln p(\mathbf{w}). \quad (31)$$

From the definition of the loss function, we obtain that the posterior is approximately Gaussian

$$f(\mathbf{w}) \propto \exp\left\{-\frac{N}{2} \mathbf{w}^T K \mathbf{w}\right\}. \quad (32)$$

The goal is to calculate the optimal learning rate which minimizes the KL divergence between the steady-state distribution $q(\mathbf{w})$ (7) obtained from SGD and the posterior (32). The KL divergence is given by

$$\begin{aligned} D_{\text{KL}}(q||f) &= -\mathbb{E}_q(\ln f) + \mathbb{E}_q(\ln q) \\ &= \frac{1}{2} [N\text{Tr}[K\Sigma] - \ln|NK| - \ln|\Sigma| - D], \end{aligned} \quad (33)$$

where $|\cdot|$ is the determinant and D is the dimension of the parameters \mathbf{w} .

We focus on the situation where the noise covariance is given by $C = \frac{N-S}{NS}K$, which is adopted by [Hoffer et al. \(2017\)](#). According to Theorem 3, the covariance of the steady distribution reads

$$\Sigma = \lambda \frac{N-S}{NS} (2I_D - \lambda K)^{-1}. \quad (34)$$

Up to constant terms, the KL divergence is given by

$$D_{\text{KL}} \stackrel{c}{=} \lambda \frac{N-S}{S} \text{Tr}[(2I_D - \lambda K)^{-1} K] - D \ln \lambda + \ln|2I_D - \lambda K| - D. \quad (35)$$

Taking the derivative with respect to λ yields

$$\frac{\partial}{\partial \lambda} D_{\text{KL}} = \frac{N-2S}{S} \text{Tr}[(2I_D - \lambda K)^{-1} K] + \lambda \frac{N-S}{S} \text{Tr}[(2I_D - \lambda K)^{-2} K^2] - \frac{D}{\lambda}. \quad (36)$$

The optimal λ is obtained by solving $\frac{\partial}{\partial \lambda} D_{\text{KL}} = 0$, namely

$$\frac{N-2S}{S} \sum_{i=1}^D \frac{k_i}{2 - \lambda k_i} + \frac{N-S}{S} \lambda \sum_{i=1}^D \frac{k_i^2}{(2 - \lambda k_i)^2} = \frac{D}{\lambda}. \quad (37)$$

This relation constitutes our general solution to this problem, which can be easily solved numerically in general. The result by [Mandt et al. \(2017\)](#) can be seen as a solution to the above set of equations after ignoring non-linear terms in λ , which gives $\lambda_c^* = 2\frac{S}{N} \frac{D}{\text{Tr}[K]}$ under the assumptions that $S \ll N$ and $\lambda k \ll 1$. With increasing λ , one requires an increasingly higher-order corrections from (37).

6.2 Escape Rate of the First Kind

Now, we investigate the effect of discreteness on the escape rate from a sharp minimum. The first indicator for the escape rate, called the escaping efficiency, is proposed by [Zhu et al. \(2019\)](#), and is defined as

$$E := \mathbb{E}[L(\mathbf{w}_t) - L(\mathbf{w}_0)], \quad (38)$$

where \mathbf{w}_0 is the exact minimum and t is a fixed time. This indicator qualitatively characterizes the ability of escape from the minimum \mathbf{w}_0 . According to the Markov inequality, the ‘‘escaping probability’’ is upper bounded by this efficiency E as

$$P(L(\mathbf{w}_t) - L(\mathbf{w}_0) \geq \delta) \leq \frac{E}{\delta}, \quad (39)$$

for any $\delta > 0$.

The continuous-time theory calculates this indicator as ([Zhu et al., 2019](#))

$$E_c = \frac{\lambda}{4} \text{Tr} [(I_D - e^{-2\lambda K t}) C]. \quad (40)$$

We can derive the same indicator directly from the discrete-time update rule (6), obtaining

$$\begin{aligned} E_d &= \frac{\lambda^2}{2} \sum_{i=0}^{t-1} \text{Tr} [CK(I_D - \lambda K)^{2i}] \\ &= \frac{\lambda}{4} \text{Tr} \left[\left(I_D - \frac{\lambda K}{2} \right)^{-1} [I_D - (I_D - \lambda K)^{2t}] C \right]. \end{aligned} \quad (41)$$

The details can be found in Appendix B. It can be shown that $E_d \geq E_c$ for all $\lambda < 2/k^*$ and $t \geq 0$ (see Appendix B for details). This suggests that the discrete theory predicts higher escape probability than the continuous one. Now we compare our result with the continuous one in two limiting cases. First, in the short-time limit, the continuous one becomes $E_c = \frac{t\lambda^2}{2} \text{Tr}[KC]$. For the discrete-time case, we consider a single step $t = 1$. The indicator is given by $E_d = \frac{\lambda^2}{2} \text{Tr}[KC]$, which is equal to the continuous one. Then, we consider the long-time limit. The continuous indicator becomes Hessian-independent: $E_c = \frac{\lambda}{4} \text{Tr}[C]$. This is a trivial result because the effect of the sharpness of the minimum is diminished. However, our discrete-time result still contains the sharpness even when the learning rate is large: $E_d = \frac{\lambda}{2} \text{Tr} [(2I_D - \lambda K)^{-1} C]$. We can clearly see that the flatter the minimum, the smaller the escaping efficiency is. If we take the small- λ limit, it recovers the trivial continuous-time result.

Following [Zhu et al. \(2019\)](#), we investigate the effect of anisotropic noise on the escape efficiency as well. We set the constraint that $\text{Tr}[C]$ is a constant for all C 's to eliminate the effect from the magnitude of noise. We consider highly anisotropic loss function and noise by assuming ill-conditioned Hessian and the noise covariance aligned with the Hessian. Specifically, we say a Hessian is *ill-conditioned*, if the eigenvalues of K , namely $k_1 \geq k_2 \cdots \geq k_D > 0$ which are in descending order, satisfy the relation $k_{l+1}, k_{l+2}, \dots, k_D < k_1 D^{-d}$ for some constant $l \ll D$ and $d > 1/2$. This condition means that only the largest l eigenvalues are relatively large. The second condition is that C is aligned with K . Let u_i be the corresponding unit eigenvector of eigenvalue k_i , for some coefficient $a > 0$, we have

$$u_1^T C u_1 \geq a k_1 \frac{\text{Tr}[C]}{\text{Tr}[K]}. \quad (42)$$

This is true if the maximal eigenvalues of C and K are aligned in proportion, namely $c_1/\text{Tr}[C] \geq a_1 k_1/\text{Tr}[K]$. The isotropic version of the noise covariance is defined as $\bar{C} := \frac{\text{Tr}[C]}{D} I_D$, which has the same magnitude as C . The continuous-time theory gives the ratio between the escaping efficiencies of these two kinds of noise by

$$\frac{\text{Tr}[KC]}{\text{Tr}[K\bar{C}]} = \mathcal{O}(aD^{2d-1}). \quad (43)$$

Our discrete-time derivation finds that this qualitative result still holds true even for long time and large learning rate. The details are given in Appendix B.

6.3 Escape Rate from a Sharp Minimum (the Kramers Problem)

In physics, the Kramers escape problem (Kramers, 1940) is to estimate the approximate mean time it takes for a particle confined in a deep well of a potential $L(w)$ to escape across the potential barrier. For continuous-time dynamics, there is a standard approach to calculate this Kramers rate (or time) (Hänggi et al., 1990). Instead of the stochastic equation for the parameter w itself, the equivalent deterministic differential equation for the probability distribution $P_c(w, t)$ (c denotes continuous-time), which is called the Fokker-Planck (FP) equation, is usually employed (Van Kampen, 2011). Specifically, the FP equation is given in a form of the continuity equation as

$$\frac{\partial P_c(w, t)}{\partial t} = -\nabla \cdot J(w, t), \quad (44)$$

where the probability current is defined as

$$\begin{aligned} J(w, t) &:= -\lambda P_c(w, t) \nabla L(w) - \mathcal{D} \nabla P_c(w, t) \\ &= \mathcal{D} \exp\left(-\frac{L(w)}{T}\right) \nabla \left[\exp\left(\frac{L(w)}{T}\right) P_c(w, t) \right]. \end{aligned} \quad (45)$$

Here $\mathcal{D} := \frac{1}{2}C$ is the diffusion matrix and T is the effective ‘‘temperature’’. The mean escape rate is defined as

$$\gamma := \frac{P(w \in V_a)}{\int_{\partial a} J \cdot dS}, \quad (46)$$

where $P(w \in V_a)$ is the probability of the particle being inside the well a , and $\int_{\partial a} J \cdot dS$ is the probability flux through the boundary of the well a . Xie et al. (2020) derived the Kramers rate from continuous-time diffusion theory. We would like to make several corrections with our discrete-time results.

For simplicity of illustration, we consider a one-dimensional model as in Figure 6(a). In continuous-time theory, the probability inside the well a can safely be approximated by 1 because the steady distribution lies almost completely within the well. However, our discrete-time theory results in a larger fluctuation in the stationary distribution. It is obvious that when λk is close to 2 the distribution spreads out. Therefore, we need to carefully calculate $P(w \in V_a)$. We approximate the width of the well a by $2\sqrt{\frac{\Delta L}{k}}$, with $\Delta L := L(b) - L(a)$ is the height of the potential barrier and b is the position of the barrier top. The probability inside a is approximated by a finite-range Gaussian integral as

$$\begin{aligned} P(w \in V_a) &= \int_{-\sqrt{\frac{\Delta L}{k}}}^{\sqrt{\frac{\Delta L}{k}}} P(w) dw \\ &= P(a) \sqrt{\frac{2\pi C}{\lambda k(2 - \lambda k)}} \operatorname{erf}\left(\sqrt{\frac{\lambda(2 - \lambda k)\Delta L}{C}}\right), \end{aligned} \quad (47)$$

where $\operatorname{erf}(z)$ is the error function. This probability is smaller than 1, which is consistent with our expectation.

For the current J , Eq. (45) can be rewritten as

$$\nabla \left[\exp\left(\frac{L(w) - L(l)}{T}\right) P_c(w) \right] = -J \mathcal{D}^{-1} \exp\left(\frac{L(w) - L(l)}{T}\right), \quad (48)$$

where l is a midpoint on the most probable escape path between a and b so that the temperature T_a dominates the path $a \rightarrow l$ and T_b dominates the path $l \rightarrow b$. In stationary state, the probability current J is a constant. It can be obtained by integrating both sides of the above equation from a to b :

$$\text{lhs} = -\exp\left(\frac{L(a) - L(l)}{T_a}\right) P_c(a), \quad (49)$$

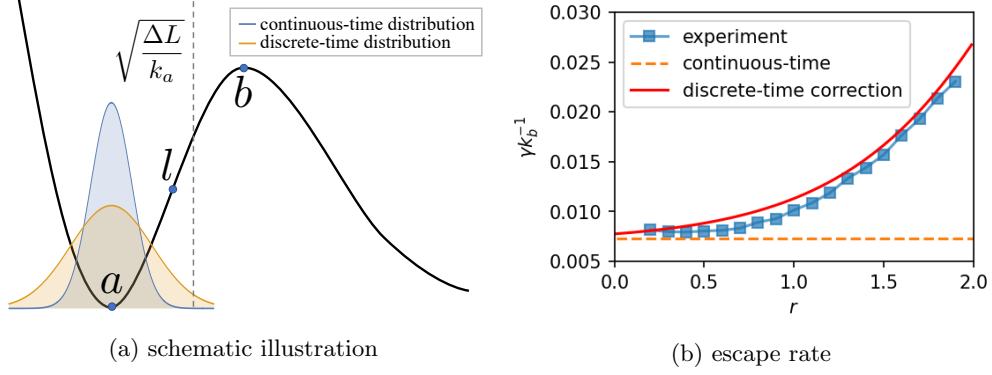


Figure 6: (a) An illustration of the Kramers problem. The stable distribution predicted by the discrete-time theory at minimum a is represented by the orange curve while the blue curve represents the continuous theory prediction. Because the discrete-time distribution spreads out of the valley, we approximate the half width of the valley a by the dashed vertical line at $\sqrt{\frac{\Delta L}{k_a}}$. (b) $\frac{\gamma}{|k_b|}$ versus r . The blue squares are taken from experiments. The orange dashed line shows the prediction of the continuous-time theory. It agrees with the experiments only for vanishingly small r . The red solid curve is our theoretical prediction multiplied by an empirical constant. Our prediction is consistent with the experimental data up to a constant coefficient.

and

$$\begin{aligned}
\text{rhs} &= -J \int_a^b \mathcal{D}^{-1} \exp\left(\frac{L(w) - L(l)}{T}\right) dw \\
&\approx -J \mathcal{D}_b^{-1} \int_{-\infty}^{\infty} \exp\left(\frac{L(b) - L(l) + \frac{1}{2}(w-b)^T k_b (w-b)}{T_b}\right) dw \\
&= -J \mathcal{D}_b^{-1} \exp\left(\frac{L(b) - L(l)}{T_b}\right) \sqrt{\frac{2\pi T_b}{|k_b|}},
\end{aligned} \tag{50}$$

where we have approximated the integrand on the right-hand side (rhs) because it is peaked around the point b . When the noise covariance is $C = \frac{1}{S} k_a$, the two “temperatures” are given by $T_a = \frac{\lambda}{2S} k_a$ and $T_b = \frac{\lambda}{2S} |k_b|$. We make two corrections to the current. First, we replace the continuous-time distribution $P_c(w)$ by the discrete-time one $P(w) = P(a) \exp(-\frac{1}{2} w^T \Sigma^{-1} w)$. Second, the effective “temperature” at point a is enlarged because the fluctuation is larger. From the distribution, the “temperature” should be $T_a = \frac{\lambda}{2S} \frac{k_a}{1 - \lambda k_a/2}$. However, we emphasize that our corrections are not precise because the current is actually a dynamical quantity. To precisely characterize it, we have to develop a discrete-time version of the FP equation (44). Hence, our corrections do not guarantee the accuracy of the coefficients in the expressions. Nevertheless, we will show that the qualitative feature and scale of our theoretical prediction are surprisingly close to the experiment in Figure 6, while the continuous-time theory simply fails.

The mean escape rate obtained from the continuous-time theory (Xie et al., 2020) is

$$\gamma_c = \frac{1}{2\pi} |k_b| \exp\left[-\frac{2S\Delta L}{\lambda} \left(\frac{l}{k_a} + \frac{1-l}{|k_b|}\right)\right]. \tag{51}$$

Our discrete-time theory gives

$$\gamma = \frac{1}{2\pi} |k_b| \sqrt{\frac{2}{2 - \lambda k_a}} \operatorname{erf}\left(\sqrt{\frac{S(2 - \lambda k_a)\Delta L}{\lambda k_a}}\right) \exp\left[-\frac{2S\Delta L}{\lambda} \left(\frac{l(1 - \lambda k_a/2)}{k_a} + \frac{1-l}{|k_b|}\right)\right]. \tag{52}$$

In Figure 6(b) we plot the quantity $\frac{\gamma}{|k_b|}$ while rescaling the loss function by a factor r : $L \rightarrow rL(w)$. Under such rescaling, the continuous-time theory predicts no change in the escape rate, whereas our theory expects a monotonic increase as r becomes large. It can be seen that such a monotonic increase is indeed observed

in experiments. The theoretical curve is rescaled by a constant factor to make the comparison easier. We see that our prediction is qualitatively consistent with the experiment, whereas the continuous-time theory is only valid in a rather limited range of small r . We expect that a real discrete-time FP equation leads to a better theoretical prediction on the Kramers rate. We leave this problem as a future project.

6.4 More on Approximation Error

In this subsection we derive the matrix equations satisfied by the steady distribution of a class of SGD with a more general form of momentum called Quasi-Hyperbolic Momentum (QHM) (Ma and Yarats, 2019; Gitman et al., 2019). The update rule is given by

$$\begin{cases} \mathbf{g}_t = K\mathbf{w}_{t-1} + \eta_{t-1}; \\ \mathbf{m}_t = \mu\mathbf{m}_{t-1} + (1-\mu)\mathbf{g}_t; \\ \mathbf{w}_t = \mathbf{w}_{t-1} - \lambda[(1-\nu)g_t + \nu\mathbf{m}_t], \end{cases} \quad (53)$$

where the additional parameter $\nu \in [0, 1]$ interpolates between the usual SGD (6) ($\nu = 0$) and a normalized version of SGD with momentum (10) ($\nu = 1$). Using the similar method in section 4.2, the covariance matrix Σ of the steady distribution is found to satisfy a set of matrix equations:

$$\begin{cases} \mu(1+\mu)(X + X^T) + \lambda[1 - \mu\nu(2 + \mu)](XK + KX^T) + a\Sigma + b(K\Sigma + \Sigma K) + cK\Sigma K = d\lambda^2 C; \\ X = (1 - \mu^2)Q + \mu\alpha K^2 \Sigma + \lambda[-1 + \mu(1 + \mu - \mu\nu)]K\Sigma K - \lambda\mu(1 - \nu)\alpha K(KQ + QK)K; \\ Q - AQA = \Sigma, \end{cases} \quad (54)$$

where

$$\begin{aligned} a &:= -2\mu(1 + \mu), & b &:= \lambda\mu^2(1 - \nu), \\ c &:= \lambda^2[1 - \mu^2 - 2\mu\nu(1 - \mu)], & d &:= \{1 + \mu[\mu - 2\nu - 2\mu\nu(1 - \nu)]\}, \\ Q &:= \sum_{i=0}^{\infty} A^i \Sigma A^i, & A &:= \mu[I_D - \lambda(1 - \nu)K], \\ \alpha &:= \lambda[1 - \nu + \nu(1 - \mu)]. \end{aligned} \quad (55)$$

By setting $\nu = 0$ and $\nu = 1$, the previous unnormalized results (8) and (16) can be recovered with reparametrization of $\lambda \rightarrow \lambda/(1 - \mu)$ (Gitman et al., 2019).

We are particularly interested in the training error $\frac{1}{2}\text{Tr}[K\Sigma]$. Extracting all the commutators as Eq. (17) in the above equations yields

$$\frac{1}{2}\text{Tr}[K\Sigma] = \frac{\lambda^2}{2}\text{Tr}[h(K)^{-1}KC], \quad (56)$$

where

$$\begin{aligned} h(K) &= \frac{\{\mu(1 + \mu)f(K) + \lambda[1 - \mu\nu(2 + \mu)]g(K)\}(I_D - A^2)^{-1} + aI_D + 2bK + cK^2}{d}, \\ f(K) &= 2(1 - \mu^2)K + \lambda[-2 + \mu[3 + \mu(2 - 3\nu)]]K^2, \\ g(K) &= 2(1 - \mu^2)I_D + 2\lambda[-1 + \mu(2 + \mu - 2\mu\nu)]K - 2\lambda\mu(1 - \nu)\alpha K^2. \end{aligned} \quad (57)$$

We emphasize that our result (56) is exact, whereas Gitman et al. (2019) only provide a low-order approximation.

6.5 Stable Distribution of Second-Order Methods

In this subsection, we deal with the stable distribution of second-order methods. We first deal with the stable distribution of Damped Newton's Method (DNM), which is the oldest and most important second-order optimization method, first invented by Newton (Nesterov, 2018). It is of interest to investigate how the second-order method behave asymptotically in a stochastic setting.

We define the learning rate as a matrix, $\Lambda := \lambda K^{-1}$. Equation (22) gives the covariance of the steady distribution as

$$\Sigma = \frac{1 + \mu}{1 - \mu} \frac{\lambda}{2(1 + \mu) - \lambda} K^{-1} C K^{-1}. \quad (58)$$

If we consider mini-batch noise, with $C = \frac{N-S}{S} K$, we have

$$\Sigma = \frac{1 + \mu}{1 - \mu} \frac{\lambda}{2(1 + \mu) - \lambda} \frac{N - S}{NS} K^{-1}. \quad (59)$$

For the approximation error, we have

$$\begin{cases} \frac{1}{2} \text{Tr}[K \Sigma_{\text{general}}] = \frac{1 + \mu}{1 - \mu} \frac{\lambda}{4(1 + \mu) - 2\lambda} \text{Tr}(K^{-1} C) \\ \frac{1}{2} \text{Tr}[K \Sigma_{\text{mini-batch}}] = \frac{1 + \mu}{1 - \mu} \frac{D\lambda}{4(1 + \mu) - 2\lambda} \frac{N - S}{NS}. \end{cases} \quad (60)$$

Next, we consider the natural gradient descent (NGD) algorithm. In traditional statistics, the efficiency of any statistical estimator is upper bounded by the celebrated Cramér-Rao's bound (CR bound) (Rao, 1992). An estimator that achieves the equality in the CR bound is said to be *Fisher-efficient*. A Fisher-efficient method is the fastest possible method to estimate a given statistical quantity. When the gradient descent is used, it is shown (Amari, 1998; Amari and Nagaoka, 2007) that if one defines the learning rate as a matrix, $\Lambda := \lambda J(\mathbf{w})^{-1}$, where $J(\mathbf{w}) := \mathbb{E}[\nabla L(\nabla L)^T]$ is the Fisher information, then this optimization algorithm becomes Fisher-efficient in the limit of $t \rightarrow \infty$. This algorithm is called the *natural gradient descent* because the Fisher information is the ‘‘natural’’ metric for measuring distance in the probability space. The NGD algorithm has therefore attracted great attention both theoretically and empirically (Pascanu and Bengio, 2013; Amari, 1998). However, previous literature often takes the continuous-time limit and nothing is known about NGD in the discrete-time regime.

We apply our formalism to derive the stable distribution of NGD in the discrete-time regime. To the best of our knowledge, this is the first work to treat the discrete-time NGD and to derive its stable distribution. Because the Fisher information is calculated as $J(\mathbf{w}) = \mathbb{E}[K \mathbf{w} \mathbf{w}^T K] = K \Sigma K$, we have $\Lambda = \lambda(K \Sigma K)^{-1}$. A substitute of this result in Eq. (22) yields the following quadratic matrix equation

$$(K \Sigma)^2 - \frac{\lambda}{2(1 + \mu)} K \Sigma - \frac{\lambda}{2(1 - \mu)} C K^{-1} = 0. \quad (61)$$

When the noise covariance C is a constant matrix which does not depend on Σ , this equation is solvable and the covariance is given by (Higham and Kim, 2001)

$$\Sigma = \frac{1}{2} K^{-1} \left[Q + \frac{\lambda}{2(1 + \mu)} I_D \right], \quad (62)$$

where $Q := \left[\frac{\lambda^2}{4(1 + \mu)^2} I_D + \frac{2\lambda}{1 - \mu} C K^{-1} \right]^{\frac{1}{2}}$. This result does not seem quite satisfying, especially because it does not seem to reduce to any meaningful distribution. This means that, when the noise is arbitrary and not related to the use of minibatch sampling, one is not recommended to use NGD⁶.

Then, we consider the case when the noise is mini-batch. When NGD is used, one should also abandon the commonly used approximate $C \approx K/S$ and use a better approximation of $C \approx \frac{N-S}{NS} \mathbb{E}[\nabla L \nabla L^T] = \frac{N-S}{NS} K \Sigma K$. Solving the equation for Σ , we obtain

$$\Sigma = \lambda \frac{(1 + \mu) \frac{N-S}{NS} + 1 - \mu}{2(1 - \mu^2)} K^{-1}. \quad (63)$$

When $S \rightarrow N$, $C = 0$, and we have $\Sigma = \frac{\lambda}{2(1 + \mu)} K^{-1}$; this means that the algorithm involves nonzero fluctuations even if the noise is absent! Moreover, the divergence caused by $\lambda k^* \rightarrow 2$ also disappears here. This suggests

⁶Recall that the NGD is derived in an online learning setting, where the noise is by definition proportional to the mini-batch noise with $N \rightarrow \infty$ and minibatch size 1 Amari (1998).

that, when the noise is mini-batch, NGD naturally corrects the ill-conditioned problem of discrete-time SGD. Even more interestingly, both the DNM and the NGD algorithms induce fluctuations that are the same as those in the continuous-time SGD algorithm with Gaussian noise up to the coefficients, in the sense that the variance is proportional to K^{-1} which is the local geometry of the minimum. Intuitively, this means that DNM and NGD need no correction even in the discrete-time case; moreover, they are likely to generalize better because they better align with the underlying loss function. For completeness, we also present the approximation error:

$$\begin{cases} \frac{1}{2} \text{Tr}[K\Sigma_{\text{general}}] = \frac{1}{4} \text{Tr} \left[Q + \frac{\lambda}{2(1+\mu)} I_D \right]; \\ \frac{1}{2} \text{Tr}[K\Sigma_{\text{mini-batch}}] = \lambda \frac{(1+\mu) \frac{N-S}{N} + 1 - \mu}{4(1-\mu^2)} D. \end{cases} \quad (64)$$

7 Concluding Remark

In this work, we have analyzed the stochastic gradient descent algorithm in a quadratic potential, which is a good approximation close to any local minimum. Our solution is exact, and relies on fewer assumptions than previous works, and, with the exact solutions, a series of corrections to those previous results that are based on continuous-time approximation can be obtained. In fact, it has been shown that, even in simple settings such as a one-dimensional quadratic loss, the prediction of the continuous-time solution may deviate arbitrarily far from the truth and is qualitatively wrong. This suggests the fundamental limitation of making the continuous-time approximation in analyzing machine learning problems. The discrete-time dynamics is more fundamental and we believe that it deserves to be dealt with directly. Previous works have shown that, SGD leads to flatter minimum due to the anisotropic noise that exists in it; this anisotropy is enhanced when the dynamics is discrete-time; this gives stronger mobility to model parameters along the sharper directions in the Hessian, and therefore, makes flatter minimum more favorable. On the other hand, the distortion that discrete-time SGD causes, in general, does not match the underlying landscape, this means that using large learning rate may cause larger approximation error and worsened generalization. This tradeoff has been solved and discussed in a restricted setting in this work, and we hope the discussions here may stimulate more research in this direction.

One of the most important problems in deep learning is to understand why deep neural networks generalize so well (Krogh and Hertz, 1992; Zhang et al., 2017; Mei and Montanari, 2019), and this may be answered in various restricted settings. For example, overparametrization definitely plays a role (Geiger et al., 2020); extrapolation properties of neural networks are also shown to be closely related to generalization (Ziyin et al., 2020); good test loss does not translate to good generalization accuracy (Chen et al., 2020); generalization may even be understood through basic economics theory (Liu et al., 2019). Using large learning rate also seems to have a close relationship with generalization. While the present work has established some fundamental properties of discrete-time SGD, the link to generalization performance is only briefly discussed. We hope that future works will fill this gap with more thorough investigations. Other interesting and related problems include mini-batch noise, which has been shown to be crucial for the generalization ability of modern deep learning models. Our experiments have shown that even in our exact solution to the discrete-time dynamics, the behavior of the mini-batch noise cannot be perfectly explained. There is more to mini-batch that requires a better solution and understanding.

From the physics point of view, learning with SGD is a non-equilibrium process (Chaudhari and Soatto, 2018). It is to ask whether and, if so, how recent developments in thermalization and non-equilibrium thermodynamics provide insights into how SGD works away from equilibrium (Ashida et al., 2020; Mori et al., 2018; Fang et al., 2019; Talkner and Hänggi, 2020; Ueda, 2020). Steady state thermodynamics (Sasa and Tasaki, 2006) and stochastic thermodynamics (Seifert, 2012) serve as tools to understand the energetics, fluctuation and dissipation for non-equilibrium steady states and general non-stationary states. Fundamental relations like thermodynamic uncertainty relations (Horowitz and Gingrich, 2019; Liu et al., 2020; Wolpert, 2020) and speed limits (Shiraishi et al., 2018) have been discovered and integrated with information theory (Ito and Dechant, 2020; Nicholson et al., 2020). It is possible that these developments lead to deeper understanding of SGD away from equilibrium. Discovering the fundamental principles behind SGD should greatly enhance our understanding about deep learning.

Acknowledgments

We acknowledge Prof. Chikara Furusawa for valuable discussions. We especially appreciate Dr. Takashi Mori for carefully reading the manuscript and providing valuable comments. Kangqiao Liu was supported by Global Science Graduate Course (GSGC) program of the University of Tokyo. Liu Ziyin thanks the department of physics and the Institute for Physics of Intelligence (IPI) of the University of Tokyo for the financial support he receives. This work was supported by KAKENHI Grant No. JP18H01145 and a Grant-in-Aid for Scientific Research on Innovative Areas “Topological Materials Science (KAKENHI Grant No. JP15H05855) from the Japan Society for the Promotion of Science.

References

- Amari, S. and Nagaoka, H. (2007). *Methods of Information Geometry*. Translations of mathematical monographs. American Mathematical Society.
- Amari, S.-I. (1998). Natural gradient works efficiently in learning. *Neural computation*, 10(2):251–276.
- Ashida, Y., Gong, Z., and Ueda, M. (2020). Non-hermitian physics. *arXiv preprint arXiv:2006.01837*.
- Bottou, L. (1999). *On-Line Learning and Stochastic Approximations*, page 9–42. Cambridge University Press, USA.
- Chaudhari, P., Choromanska, A., Soatto, S., LeCun, Y., Baldassi, C., Borgs, C., Chayes, J., Sagun, L., and Zecchina, R. (2019). Entropy-sgd: Biasing gradient descent into wide valleys. *Journal of Statistical Mechanics: Theory and Experiment*, 2019(12):124018.
- Chaudhari, P. and Soatto, S. (2018). Stochastic gradient descent performs variational inference, converges to limit cycles for deep networks. In *2018 Information Theory and Applications Workshop (ITA)*, pages 1–10.
- Chen, B., Ziyin, L., Wang, Z., and Liang, P. P. (2020). An investigation of how label smoothing affects generalization. *arXiv preprint arXiv:2010.12648*.
- Chizat, L. and Bach, F. (2018). A note on lazy training in supervised differentiable programming. *arXiv preprint arXiv:1812.07956*, 8.
- Duchi, J., Hazan, E., and Singer, Y. (2011). Adaptive subgradient methods for online learning and stochastic optimization. *J. Mach. Learn. Res.*, 12(null):2121–2159.
- Dziugaite, G. K. and Roy, D. M. (2017). Computing nonvacuous generalization bounds for deep (stochastic) neural networks with many more parameters than training data.
- Einstein, A. (2005). Über die von der molekularkinetischen theorie der wärme geforderte bewegung von in ruhenden flüssigkeiten suspendierten teilchen [adp 17, 549 (1905)]. *Annalen der Physik*, 14(S1):182–193.
- Fang, X., Kruse, K., Lu, T., and Wang, J. (2019). Nonequilibrium physics in biology. *Rev. Mod. Phys.*, 91:045004.
- Flammarion, N. and Bach, F. (2015). From averaging to acceleration, there is only a step-size. volume 40 of *Proceedings of Machine Learning Research*, pages 658–695, Paris, France. PMLR.
- Funo, K., Ueda, M., and Sagawa, T. (2018). Quantum fluctuation theorems. In *Thermodynamics in the Quantum Regime*, pages 249–273. Springer.
- Geiger, M., Jacot, A., Spigler, S., Gabriel, F., Sagun, L., d’Ascoli, S., Biroli, G., Hongler, C., and Wyart, M. (2020). Scaling description of generalization with number of parameters in deep learning. *Journal of Statistical Mechanics: Theory and Experiment*, 2020(2):023401.
- Gitman, I., Lang, H., Zhang, P., and Xiao, L. (2019). Understanding the role of momentum in stochastic gradient methods. In *Advances in Neural Information Processing Systems*, pages 9633–9643.
- Goodfellow, I., Bengio, Y., and Courville, A. (2016). *Deep Learning*. MIT Press. <http://www.deeplearningbook.org>.

- Goyal, P., Dollár, P., Girshick, R., Noordhuis, P., Wesolowski, L., Kyrola, A., Tulloch, A., Jia, Y., and He, K. (2017). Accurate, large minibatch sgd: Training imagenet in 1 hour. *arXiv preprint arXiv:1706.02677*.
- Hänggi, P., Talkner, P., and Borkovec, M. (1990). Reaction-rate theory: fifty years after kramers. *Rev. Mod. Phys.*, 62:251–341.
- Hanin, B. and Nica, M. (2019). Finite depth and width corrections to the neural tangent kernel. *arXiv preprint arXiv:1909.05989*.
- He, K., Zhang, X., Ren, S., and Sun, J. (2016). Deep residual learning for image recognition. In *2016 IEEE Conference on Computer Vision and Pattern Recognition (CVPR)*, pages 770–778.
- Higham, N. J. and Kim, H.-M. (2001). Solving a quadratic matrix equation by newton’s method with exact line searches. *SIAM Journal on Matrix Analysis and Applications*, 23(2):303–316.
- Hinton, G., Deng, L., Yu, D., Dahl, G. E., Mohamed, A., Jaitly, N., Senior, A., Vanhoucke, V., Nguyen, P., Sainath, T. N., and Kingsbury, B. (2012). Deep neural networks for acoustic modeling in speech recognition: The shared views of four research groups. *IEEE Signal Processing Magazine*, 29(6):82–97.
- Hoffer, E., Hubara, I., and Soudry, D. (2017). Train longer, generalize better: closing the generalization gap in large batch training of neural networks. In Guyon, I., Luxburg, U. V., Bengio, S., Wallach, H., Fergus, R., Vishwanathan, S., and Garnett, R., editors, *Advances in Neural Information Processing Systems 30*, pages 1731–1741. Curran Associates, Inc.
- Horowitz, J. M. and Gingrich, T. R. (2019). Thermodynamic uncertainty relations constrain non-equilibrium fluctuations. *Nat. Phys.*
- Hu, W., Li, C. J., Li, L., and Liu, J.-G. (2018). On the diffusion approximation of nonconvex stochastic gradient descent.
- Ito, S. and Dechant, A. (2020). Stochastic time evolution, information geometry, and the cramér-rao bound. *Phys. Rev. X*, 10:021056.
- Jacot, A., Gabriel, F., and Hongler, C. (2018). Neural tangent kernel: Convergence and generalization in neural networks. In Bengio, S., Wallach, H., Larochelle, H., Grauman, K., Cesa-Bianchi, N., and Garnett, R., editors, *Advances in Neural Information Processing Systems 31*, pages 8571–8580. Curran Associates, Inc.
- Jastrzebski, S., Kenton, Z., Arpit, D., Ballas, N., Fischer, A., Bengio, Y., and Storkey, A. (2018). Three factors influencing minima in sgd.
- Jiang*, Y., Neyshabur*, B., Mobahi, H., Krishnan, D., and Bengio, S. (2020). Fantastic generalization measures and where to find them. In *International Conference on Learning Representations*.
- Kingma, D. P. and Ba, J. (2017). Adam: A method for stochastic optimization.
- Kramers, H. (1940). Brownian motion in a field of force and the diffusion model of chemical reactions. *Physica*, 7(4):284 – 304.
- Krizhevsky, A., Sutskever, I., and Hinton, G. E. (2017). Imagenet classification with deep convolutional neural networks. *Commun. ACM*, 60(6):84–90.
- Krogh, A. and Hertz, J. A. (1992). Generalization in a linear perceptron in the presence of noise. *Journal of Physics A: Mathematical and General*, 25(5):1135.
- Kubo, R. (1966). The fluctuation-dissipation theorem. *Reports on progress in physics*, 29(1):255.
- LeCun, Y. A., Bottou, L., Orr, G. B., and Müller, K.-R. (2012). *Efficient BackProp*, pages 9–48. Springer Berlin Heidelberg, Berlin, Heidelberg.
- Lee, J., Xiao, L., Schoenholz, S. S., Bahri, Y., Novak, R., Sohl-Dickstein, J., and Pennington, J. (2019). Wide neural networks of any depth evolve as linear models under gradient descent.

- Lewkowycz, A., Bahri, Y., Dyer, E., Sohl-Dickstein, J., and Gur-Ari, G. (2020). The large learning rate phase of deep learning: the catapult mechanism.
- Li, Q., Tai, C., and E, W. (2017). Stochastic modified equations and adaptive stochastic gradient algorithms. volume 70 of *Proceedings of Machine Learning Research*, pages 2101–2110, International Convention Centre, Sydney, Australia. PMLR.
- Li, Y., Wei, C., and Ma, T. (2019). Towards explaining the regularization effect of initial large learning rate in training neural networks. *ArXiv*, abs/1907.04595.
- Liang, T., Poggio, T., Rakhlin, A., and Stokes, J. (2019). Fisher-rao metric, geometry, and complexity of neural networks.
- Liu, K., Gong, Z., and Ueda, M. (2020). Thermodynamic uncertainty relation for arbitrary initial states. *Phys. Rev. Lett.*, 125:140602.
- Liu, Z., Wang, Z., Liang, P. P., Salakhutdinov, R. R., Morency, L.-P., and Ueda, M. (2019). Deep gamblers: Learning to abstain with portfolio theory. In *Advances in Neural Information Processing Systems*, pages 10623–10633.
- Luong, T., Pham, H., and Manning, C. D. (2015). Effective approaches to attention-based neural machine translation. In *Proceedings of the 2015 Conference on Empirical Methods in Natural Language Processing*, pages 1412–1421, Lisbon, Portugal. Association for Computational Linguistics.
- Ma, J. and Yarats, D. (2019). Quasi-hyperbolic momentum and adam for deep learning. In *International Conference on Learning Representations*.
- Ma, Y.-A., Chen, T., and Fox, E. B. (2015). A complete recipe for stochastic gradient mcmc. In *Proceedings of the 28th International Conference on Neural Information Processing Systems - Volume 2*, NIPS’15, page 2917–2925, Cambridge, MA, USA. MIT Press.
- MacKay, D. J. C. (1992). A practical bayesian framework for backpropagation networks. *Neural Computation*, 4(3):448–472.
- Mandt, S., Hoffman, M. D., and Blei, D. M. (2017). Stochastic gradient descent as approximate bayesian inference. *J. Mach. Learn. Res.*, 18(1):4873–4907.
- Mei, S. and Montanari, A. (2019). The generalization error of random features regression: Precise asymptotics and double descent curve. *arXiv preprint arXiv:1908.05355*.
- Mori, T., Ikeda, T. N., Kaminishi, E., and Ueda, M. (2018). Thermalization and prethermalization in isolated quantum systems: a theoretical overview. *Journal of Physics B: Atomic, Molecular and Optical Physics*, 51(11):112001.
- Mori, T. and Ueda, M. (2020a). Improved generalization by noise enhancement.
- Mori, T. and Ueda, M. (2020b). Is deeper better? it depends on locality of relevant features.
- Nagarajan, V. and Kolter, J. Z. (2019). Generalization in deep networks: The role of distance from initialization.
- Nesterov, Y. (2018). *Lectures on convex optimization*, volume 137. Springer.
- Neysshabur, B., Bhojanapalli, S., McAllester, D., and Srebro, N. (2017). Exploring generalization in deep learning. In *Proceedings of the 31st International Conference on Neural Information Processing Systems*, NIPS’17, page 5949–5958, Red Hook, NY, USA. Curran Associates Inc.
- Neysshabur, B., Bhojanapalli, S., and Srebro, N. (2018). A PAC-bayesian approach to spectrally-normalized margin bounds for neural networks. In *International Conference on Learning Representations*.
- Nicholson, S. B., García-Pintos, L. P., del Campo, A., and Green, J. R. (2020). Time–information uncertainty relations in thermodynamics. *Nature Physics*.
- Pascanu, R. and Bengio, Y. (2013). Revisiting natural gradient for deep networks. *arXiv preprint arXiv:1301.3584*.
- Rao, C. R. (1992). Information and the accuracy attainable in the estimation of statistical parameters. In *Breakthroughs in statistics*, pages 235–247. Springer.

- Rissanen, J. (1983). A universal prior for integers and estimation by minimum description length. *Ann. Statist.*, 11(2):416–431.
- Sasa, S.-i. and Tasaki, H. (2006). Steady state thermodynamics. *Journal of Statistical Physics*, 125(1):125–224.
- Seifert, U. (2012). Stochastic thermodynamics, fluctuation theorems and molecular machines. *Reports on Progress in Physics*, 75(12):126001.
- Shiraishi, N., Funo, K., and Saito, K. (2018). Speed limit for classical stochastic processes. *Phys. Rev. Lett.*, 121:070601.
- Shirish Keskar, N., Mudigere, D., Nocedal, J., Smelyanskiy, M., and Tang, P. T. P. (2016). On Large-Batch Training for Deep Learning: Generalization Gap and Sharp Minima. *ArXiv e-prints*.
- Smith, S. L. and Le, Q. V. (2017). A bayesian perspective on generalization and stochastic gradient descent. *arXiv preprint arXiv:1710.06451*.
- Sutskever, I., Martens, J., Dahl, G., and Hinton, G. (2013). On the importance of initialization and momentum in deep learning. volume 28 of *Proceedings of Machine Learning Research*, pages 1139–1147, Atlanta, Georgia, USA. PMLR.
- Talkner, P. and Hänggi, P. (2020). Colloquium: Statistical mechanics and thermodynamics at strong coupling: Quantum and classical. *Rev. Mod. Phys.*, 92:041002.
- Talkner, P., Hänggi, P., Freidkin, E., and Trautmann, D. (1987). Discrete dynamics and metastability: Mean first passage times and escape rates. *Journal of Statistical Physics*, 48(1):231–254.
- Ueda, M. (2020). Quantum equilibration, thermalization and prethermalization in ultracold atoms. *Nature Reviews Physics*, pages 1–13.
- Van Kampen, N. (2011). *Stochastic Processes in Physics and Chemistry*. North-Holland Personal Library. Elsevier Science.
- Vapnik, V. N. and Chervonenkis, A. Y. (1971). On the uniform convergence of relative frequencies of events to their probabilities. *Theory of Probability & Its Applications*, 16(2):264–280.
- Welling, M. and Teh, Y. W. (2011). Bayesian learning via stochastic gradient langevin dynamics. In *Proceedings of the 28th International Conference on International Conference on Machine Learning*, ICML’11, page 681–688, Madison, WI, USA. Omnipress.
- Wilson, A. C., Roelofs, R., Stern, M., Srebro, N., and Recht, B. (2017). The marginal value of adaptive gradient methods in machine learning. In *Advances in Neural Information Processing Systems*, pages 4148–4158.
- Wolpert, D. H. (2020). Uncertainty relations and fluctuation theorems for bayes nets. *Phys. Rev. Lett.*, 125:200602.
- Wu, L., Ma, C., and E, W. (2018). How sgd selects the global minima in over-parameterized learning: A dynamical stability perspective. In Bengio, S., Wallach, H., Larochelle, H., Grauman, K., Cesa-Bianchi, N., and Garnett, R., editors, *Advances in Neural Information Processing Systems 31*, pages 8279–8288. Curran Associates, Inc.
- Xie, Z., Sato, I., and Sugiyama, M. (2020). A diffusion theory for deep learning dynamics: Stochastic gradient descent exponentially favors flat minima.
- Xu, G., Wei, M., and Zheng, D. (1998). On solutions of matrix equation $axb + cyd = f$. *Linear Algebra and its Applications*, 279(1):93 – 109.
- Yaida, S. (2018). Fluctuation-dissipation relations for stochastic gradient descent. *arXiv preprint arXiv:1810.00004*.
- Zhang, C., Bengio, S., Hardt, M., Recht, B., and Vinyals, O. (2017). Understanding deep learning requires rethinking generalization.
- Zhu, Z., Wu, J., Yu, B., Wu, L., and Ma, J. (2019). The anisotropic noise in stochastic gradient descent: Its behavior of escaping from sharp minima and regularization effects. volume 97 of *Proceedings of Machine Learning Research*, pages 7654–7663, Long Beach, California, USA. PMLR.
- Ziyin, L., Hartwig, T., and Ueda, M. (2020). Neural networks fail to learn periodic functions and how to fix it. *Advances in Neural Information Processing Systems*, 33.

A Proof to Lemma 1.

We introduce simplified notations: $X := (1 - \mu)I_D$ and $Y := I_D - \lambda K$. By iteration, we have

$$\begin{aligned} \mathbf{w}_t &= (X + Y)\mathbf{w}_{t-1} - X\mathbf{w}_{t-2} + \lambda\eta_{t-1} \\ &\dots \\ &= g_{t-1}\mathbf{w}_1 - Xg_{t-2}\mathbf{w}_0 + \lambda \sum_{i=0}^{t-1} g_i\eta_{t-1-i}, \end{aligned} \quad (65)$$

where the coefficient matrices g_i satisfy the following recurrence relation

$$g_t = (X + Y)g_{t-1} - Xg_{t-2}, \quad \text{for } t \geq 2, \quad (66)$$

with initial terms given by

$$g_0 = I_D, \quad g_1 = X + Y. \quad (67)$$

It can be seen that $\lim_{t \rightarrow \infty} g_t = 0$. Hence, we have

$$\begin{aligned} \lim_{t \rightarrow \infty} \mathbf{w}_t &= \lim_{t \rightarrow \infty} \lambda \sum_{i=0}^{t-1} g_i\eta_{t-1-i} \\ &\sim \mathcal{N}\left(0, \lambda^2 \lim_{t \rightarrow \infty} \sum_{i=0}^{t-1} g_i C g_i\right) \\ &:= \mathcal{N}(0, \Sigma). \end{aligned} \quad (68)$$

Because every g_i is a function of K , $[C, K] = 0$ is equivalent with $[\Sigma, K] = 0$.

B Derivations in Section 6.2

We first derive the discrete-time version of the escaping efficiency (41). Because the initial state is the exact minimum, namely $\mathbf{w}_0 = 0$, at time t the parameters evolve to

$$\mathbf{w}_t = \lambda \sum_{i=0}^{t-1} (I_D - \lambda K)^i \eta_{t-1-i}. \quad (69)$$

The loss function is therefore given by

$$L(\mathbf{w}_t) = \frac{\lambda^2}{2} \sum_{i=0}^{t-1} \eta_{t-1-i}^T K (I_D - \lambda K)^{2i} \eta_{t-1-i} + \text{crossterms}. \quad (70)$$

Taking the expectation yields

$$E := \mathbb{E}[L(\mathbf{w}_t)] = \frac{1}{2} \sum_{i=0}^{t-1} \text{Tr}[CK(I_D - \lambda K)^{2i}], \quad (71)$$

where the cross terms vanish due to the Gaussian property of the noise. For a single step $t = 1$, we obtain

$$E = \frac{\lambda^2}{2} \text{Tr}[KC]. \quad (72)$$

In long-time limit, according to the Neumann series, we obtain

$$E = \frac{\lambda}{2} \text{Tr}[(2I_D - \lambda K)^{-1}C]. \quad (73)$$

Next, we prove that $E_d \geq E_c$ for all $\lambda < 2/k^*$ and $t \geq 0$. As a necessary condition, if each component inside the trace of E_d is greater than that of E_c , the trace itself should be so as well. Specifically, we would like to show that

$$\left(1 - \frac{\lambda k}{2}\right)^{-1} \left[1 - (1 - \lambda k)^{2t}\right] \geq 1 - e^{-2\lambda k t}, \quad \forall 0 < \lambda k < 2 \text{ and } t \geq 0. \quad (74)$$

Equivalently, we want to show that

$$\left(1 - \frac{\lambda k}{2}\right) e^{-2\lambda k t} \geq (1 - \lambda k)^{2t} - \frac{\lambda k}{2}. \quad (75)$$

Because $e^{-x} \geq 1 - x$ for all $x \geq 0$, we have

$$\text{lhs} \geq \left(1 - \frac{\lambda k}{2}\right) (1 - \lambda k)^{2t} = (1 - \lambda k)^{2t} - \frac{\lambda k}{2} (1 - \lambda k)^{2t} \geq (1 - \lambda k)^{2t} - \frac{\lambda k}{2} = \text{rhs}. \quad \square \quad (76)$$

Then, we derive the second condition about the alignment assumption. We denote the maximal eigenvalue and the corresponding eigenvector of C as c_1 and v_1 , respectively. We have $u_1^T C u_1 \geq u_1^T v_1 c_1 v_1^T u_1 = c_1 \langle u_1, v_1 \rangle^2$. If the maximal eigenvalues of C and K are aligned in proportion, namely $c_1/\text{Tr}[C] \geq a_1 k_1/\text{Tr}[K]$, and the angle between their eigenvectors is so small that $\langle u_1, v_1 \rangle^2 \geq a_2$, then we can conclude that $u_1^T C u_1 \geq a k_1 \frac{\text{Tr}[C]}{\text{Tr}[K]}$ with $a := a_1 a_2$.

Finally, we derive the efficiency ratio (43). First, for a single step it is the same as the continuous-time one. Decomposing $\text{Tr}[KC]$, we have

$$\text{Tr}[KC] = \sum_{i=1}^D k_i u_i^T C u_i \geq k_1 u_1^T C u_1 \geq a k_1^2 \frac{\text{Tr}[C]}{\text{Tr}[K]}. \quad (77)$$

For the isotropic equivalence of the noise, we have

$$\text{Tr}[K\bar{C}] = \frac{\text{Tr}[C]}{D} \text{Tr}[K]. \quad (78)$$

Therefore, we obtain

$$\frac{\text{Tr}[KC]}{\text{Tr}[K\bar{C}]} \geq aD \frac{k_1^2}{(\text{Tr}[K])^2} \geq aD \frac{k_1^2}{[lk_1 + (D-l)D^{-d}k_1]^2} \approx aD \frac{1}{[l + (D-l)D^{-d}]^2} = \mathcal{O}(aD^{2d-1}). \quad (79)$$

Next, for long time, the alignment argument should be slightly modified. While the order of eigenvalues of K is the same as that of $(2I_D - \lambda K)^{-1}$ and they share the same set of eigenvectors, the only thing that should be modified in the argument is that the maximal eigenvalues of C and $(2I_D - \lambda K)^{-1}$ are aligned in proportion such that

$$\frac{c_1}{\text{Tr}[C]} \geq a_3 \frac{(2 - \lambda k_1)^{-1}}{\text{Tr}[(2I_D - \lambda K)^{-1}]}, \quad (80)$$

where a_3 is different from a_1 in general. Then final ratio should contain $a' := a_3 a_2$, instead of $a = a_1 a_2$. The remaining derivation is the same as above.